nature genetics

Genome-wide association study identifies five new susceptibility loci for primary angle closure glaucoma

Primary angle closure glaucoma (PACG) is a major cause of blindness worldwide. We conducted a genome-wide association study (GWAS) followed by replication in a combined total of 10,503 PACG cases and 29,567 controls drawn from 24 countries across Asia, Australia, Europe, North America, and South America. We observed significant evidence of disease association at five new genetic loci upon meta-analysis of all patient collections. These loci are at *EPDR1* rs3816415 (odds ratio (OR) = 1.24, $P = 5.94 \times 10^{-15}$), *CHAT* rs1258267 (OR = 1.22, $P = 2.85 \times 10^{-16}$), *GLIS3* rs736893 (OR = 1.18, $P = 1.43 \times 10^{-14}$), *FERMT2* rs7494379 (OR = 1.14, $P = 3.43 \times 10^{-11}$), and *DPM2–FAM102A* rs3739821 (OR = 1.15, $P = 8.32 \times 10^{-12}$). We also confirmed significant association at three previously described loci ($P < 5 \times 10^{-8}$ for each sentinel SNP at *PLEKHA7*, *COL11A1*, and *PCMTD1–ST18*)[1], providing new insights into the biology of PACG.

Glaucoma is the most common cause of irreversible blindness worldwide[2]. The main forms of glaucoma are primary open angle glaucoma (POAG), PACG, and exfoliation glaucoma. All three forms of glaucoma show familial clustering, suggesting a substantial genetic component in pathogenesis. Recent genetic studies have implicated several distinct loci associated with each of these types of glaucoma[1,3–6]. For PACG, the epidemiological risk factors include advancing age, female sex, and East Asian ancestry[7,8]. Up to 80% of the estimated 15 million people afflicted with PACG live in Asia[9], where the disease is responsible for a high proportion of blindness[10–13]. Patients either present with acute primary angle closure (APAC) or have PACG upon presentation (**Supplementary Note**). We previously performed a GWAS of PACG susceptibility on 1,854 PACG cases and 9,608 controls with replication in 1,917 cases and 8,943 controls, identifying three susceptibility loci[1].

We now expand the study to perform a discovery-stage GWAS on a combined total of 6,525 PACG cases and 19,929 controls, which were enrolled from 15 countries spanning East Asia, South Asia, Europe, and South America (**Fig. 1** and **Supplementary Table 1**). We applied routine quality control checks for SNPs and samples as is usually done for GWAS analyses (Online Methods). SNPs at ten distinct loci surpassed $P < 1 \times 10^{-6}$ (**Supplementary Table 2**), a threshold we took to be indicative of suggestive evidence of association with disease[14]. Three of these loci have previously been reported (**Fig. 2** and **Supplementary Table 3**)[1]. We then subjected the ten sentinel SNPs representing each of the ten independent loci to replication genotyping in a further 3,978 cases and 9,638 controls from 14 countries (**Supplementary Table 1**). Significant replication was observed at eight distinct loci (**Table 1** and **Supplementary Table 2**; the initial associations observed at *FNDC3B* rs16856870 on chromosome 3 and *SLC38A6* rs10483730 on chromosome 14 did not replicate), and meta-analysis of all discovery and replication samples totaling 10,503 PACG cases and 29,567 controls showed genome-wide significant evidence of association for the eight loci with PACG (**Fig. 2** and **Table 1**). This two-stage study design is powered to detect effect sizes as low as 1.15 with minor allele frequencies (MAFs) as low as 0.15 at genome-wide significance (**Supplementary Table 4**).

We next asked whether heterogeneity in genetic effect sizes exists across ancestry groups and geographical locations and found that only *EPDR1* rs3816415 showed discernable evidence of heterogeneity in the overall meta-analysis ($P_{het} = 0.0072$, I^2 index = 43.0%). Closer scrutiny showed that effect sizes were consistently larger in Europeans (OR = 1.42) than in Asians (OR = 1.21) (**Fig. 3** and **Table 1**), despite similar risk allele frequencies across the ancestry groups (**Supplementary Table 5**). This discrepancy could be due either to more unreliable estimation in Europeans because of the smaller sample size in comparison to Asians (n = 1,105 European PACG cases versus 9,398 Asian PACG cases) or to a genuine difference in effect between Asians and Europeans[15–17]. We did not observe significant heterogeneity in effect sizes at the other four loci (**Fig. 3** and **Table 1**). Imputation-based fine-mapping and regional association analysis showed that each SNP locus mapped distinctly among its nearest genes, mostly framed by recombination events (**Supplementary Fig. 1**). However, as the GWAS approach assays mostly common, representative genetic variants across the human genome, we are unable to exclude the possibility that the identified SNPs at each locus could be tagging functional variants that are exerting control on distant gene targets in a position- and orientation-independent manner[18,19].

We next examined the ocular expression of genes located in the newly identified PACG loci by RT–PCR. We detected mRNA expression of *EPDR1*, *GLIS3*, *FERMT2*, *DPM2*, *PIP5KL1*, and *FAM102A* in human ocular anterior segment tissues such as the iris, ciliary body, and trabecular meshwork (**Supplementary Fig. 2a**). We also observed mRNA expression of all six genes in the cornea, lens, retina, choroid, optic nerve head, and optic nerve. We also investigated the distribution of the encoded proteins of these genes in ocular tissues by immunohistochemical labeling of sections of a normal human eye (**Supplementary Figs. 3–9**), testing for tissue specificity of expression through immunoblot analysis in ocular-tissue-derived cell lines

A full list of authors and affiliations appear at the end of the paper.

Received 7 November 2015; accepted 7 March 2016; published online 4 April 2016; doi:10.1038/ng.3540

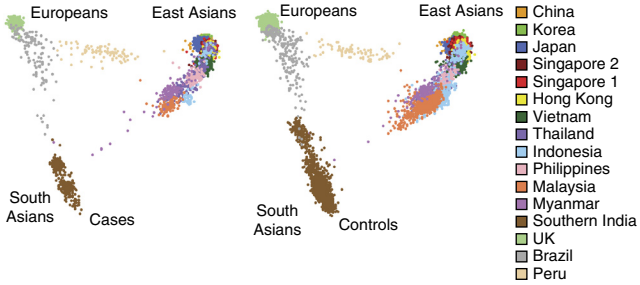

Figure 1 Distribution of PACG cases and controls from the GWAS discovery stage, which encompassed collections from 15 countries. Cases and controls are projected onto the top two principal components of genetic stratification, with cases on the left and controls on the right. Principal-component comparisons for each of the East Asian countries are shown in **Supplementary Figure 10**.

(**Supplementary Fig. 2b–h**). Overall, protein expression and localization corroborated the mRNA data, except in the case of GLIS3, where pronounced protein expression was seen in the iris, different to what was observed in mRNA expression analysis (**Supplementary Fig. 2a**). This difference may be attributed to the insensitivity of the RT–PCR technique for transcripts present at low levels.

EPDR1 encodes a glycosylated type II transmembrane protein known as ependymin-related 1. It potentially has a role in cell adhesion, as it is similar to protocadherins and ependymins[20]. SNP *EPDR1* rs16879765 has been shown to be significantly associated with Dupuytren's contracture, an inherited disorder of connective tissues[21]. Our genome-wide significant association at *EPDR1* for PACG is marked by the sentinel SNP rs3816415, which is very poorly correlated with rs16879765 despite being located less than 1 kb away. This pleiotropic association with *EPDR1* merits further study and highlights the relevance of cell adhesion molecules more broadly in PACG pathology.

SNP rs3739821 is located in an intergenic region between *DPM2* and *FAM102A*, a gene yet to be fully characterized. Mutations in *DPM2* have been linked to congenital defects in glycosylation[22], leading to severe neurological phenotypes. Although not much is known about *FAM102A* except that its expression is sensitive to the addition of β-estradiol[23], the nearby *PIP5KL1* gene (**Supplementary Fig. 1**) has been reported to be involved in cell proliferation[24] and potentially in tumorigenesis. Our expression analysis showed that all three genes (*FAM102A*, *DPM2*, and *PIP5KL1*) were expressed in all eye tissues tested, thus providing biological support for their involvement in PACG (**Supplementary Figs. 2** and **7–9**). Further fine-mapping work is needed to identify the causative gene in this locus.

CHAT on chromosome 10 encodes choline acetyltransferase. This is an enzyme responsible for synthesis of the neurotransmitter acetylcholine, which has a role in pupillary constriction. Anticholinergic medications can precipitate acute PACG via pupillary dilatation and subsequent pupillary block[25,26]. Therefore, it is plausible that natural genetic variation in a gene influencing acetylcholine metabolism could influence risk for PACG.

FERMT2 encodes a protein called pleckstrin-homology-domain-containing family C member 1 (PLEKHC1), a component of the extracellular matrix, and could thus have a role in cell adhesion[27]. PLEKHC1 belongs to the same pleckstrin family of proteins as PLEKHA7, and we previously showed that common SNPs mapping to *PLEKHA7* are significantly associated with susceptibility to PACG[1]. Our current observation of genome-wide significant associations at *FERMT2* and *EPDR1*, as well as the previous report of *PLEKHA7*, strongly implicates the cell–cell adhesion process as being important in the pathogenesis of PACG.

GLIS3 is a member of the GLI-similar subfamily of Krüppel-like zinc-finger proteins[28]. Earlier studies have shown that mutations in *GLIS3* cause neonatal diabetes and congenital hypothyroidism[29]. SNP markers mapping close to *GLIS3* have been observed to be significantly associated with type 1 diabetes in Europeans (rs7020673)[30], type 2 diabetes in East Asians (rs7041847)[31], and fasting plasma glucose levels in a large meta-analysis of European collections (rs7034200)[32]. These SNPs are independent from rs736893, which we observe here to be associated with PACG. These observations implicate yet unknown metabolic pathways that could contribute to PACG pathogenesis.

We next looked up reported loci showing genome-wide significant association with POAG[3,4,33,34] in our PACG discovery GWAS data set, as susceptibility variants for the two common forms of glaucoma could potentially be shared. We observed evidence of association at *ARHGEF12* rs2276035 and *GAS7* rs12150284. For both loci, the direction of effect was consistent in PACG and POAG (**Supplementary Table 6**). Reciprocally, we also assessed all eight genome-wide significant PACG loci in 968 POAG cases and 3,916 controls of Singaporean Chinese descent[35] but did not observe consistent evidence of association between the PACG loci and POAG (**Supplementary Table 7**).

Both ocular axial length and anterior chamber depth have previously been reported as anatomical risk factors for PACG, whereby individuals with eyes having less anterior chamber depth and shorter axial length are at increased risk of PACG[36]. We examined the six loci associated with axial length at

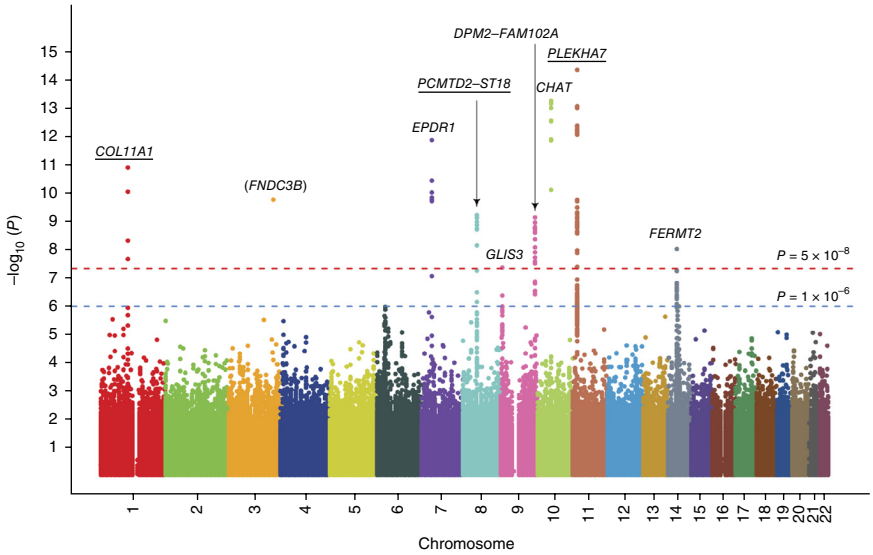

Figure 2 Results of the discovery GWAS meta-analysis. The three previously reported loci are underlined. *FNDC3B* did not replicate in the replication collections. SNPs at *EPDR1*, *GLIS3*, *DPM2–FAM102A*, *CHAT*, and *FERMT2* represent new genome-wide significant associations.

Table 1 Results for the eight genome-wide significant loci upon meta-analysis of all PACG case–control collections

SNP (risk/reference)	Chr.	Position (bp)	Gene locus	Stage	Per-allele OR	*P*	P_{het}	I^2 index (%)
New loci								
rs3816415 (A/G)	7	37,988,311	*EPDR1*	GWAS	1.28	1.28×10^{-12}	0.6	0
				Replication	1.17	0.00032	0.0013	60.4
				All-data meta-analysis	1.24	5.94×10^{-15}	0.0072	43.0
				Asian descent	1.21	7.49×10^{-11}	0.095	29.1
				European descent	1.42	1.86×10^{-6}	0.029	55.3
rs736893 (G/A)	9	4,217,028	*GLIS3*	GWAS	1.16	4.23×10^{-8}	0.85	0
				Replication	1.20	4.64×10^{-8}	0.48	0
				All-data meta-analysis	1.18	1.43×10^{-14}	0.78	0
				Asian descent	1.17	1.2×10^{-11}	0.57	0
				European descent	1.25	0.00015	0.94	0
rs3739821 (G/A)	9	130,702,477	*DPM2–FAM102A*	GWAS	1.17	7.08×10^{-10}	0.93	0
				Replication	1.11	0.0013	0.28	15.7
				All-data meta-analysis	1.15	8.32×10^{-12}	0.62	0
				Asian descent	1.15	4.5×10^{-11}	0.46	0
				European descent	1.12	0.06	0.79	0
rs1258267 (A/G)	10	50,895,770	*CHAT*	GWAS	1.25	5.06×10^{-14}	0.59	0
				Replication	1.16	0.00046	0.57	0
				All-data meta-analysis	1.22	2.85×10^{-16}	0.58	0
				Asian descent	1.22	4.99×10^{-16}	0.58	0
				European descent	1.43	0.24[a]	0.32	14.2
rs7494379 (G/A)	14	53,411,391	*FERMT2*	GWAS	1.15	9.26×10^{-9}	0.56	0
				Replication	1.11	0.00065	0.24	19.2
				All-data meta-analysis	1.14	3.43×10^{-11}	0.39	5.0
				Asian descent	1.13	5.42×10^{-9}	0.36	7.3
				European descent	1.22	0.00066	0.52	0
Previously reported loci								
rs3753841 (G/A)	1	103,379,918	*COL11A1*	GWAS	1.18	1.18×10^{-11}	0.32	11.4
				Replication	1.29	1.15×10^{-14}	0.47	0
				All-data meta-analysis	1.21	1.27×10^{-23}	0.21	16.8
				Asian descent	1.21	4×10^{-21}	0.35	8.1
				European descent	1.20	0.00076	0.099	42.0
rs1015213 (A/G)	8	52,887,541	*PCMTD1–ST18*	GWAS	1.44	1.75×10^{-9}	0.21	21.2
				Replication	1.40	5.47×10^{-8}	0.51	0
				All-data meta-analysis	1.42	5.42×10^{-16}	0.34	8.0
				Asian descent	1.44	1.68×10^{-13}	0.096	29
				European descent	1.35	0.0006	0.99	0
rs11024102 (G/A)	11	17,008,605	*PLEKHA7*	GWAS	1.20	4.1×10^{-15}	0.77	0
				Replication	1.15	5.51×10^{-5}	0.48	0
				All-data meta-analysis	1.18	1.93×10^{-18}	0.71	0
				Asian descent	1.20	8×10^{-19}	0.87	0
				European descent	1.05	0.38	0.54	0

All SNPs reported here were directly genotyped on the GWAS arrays. Chr., chromosome.
[a]The minor allele for *CHAT* rs1258267 is very rare in Europeans (**Supplementary Table 5**). Of the six European-ancestry populations (Australia, Brazil, Peru, Poland, UK, and United States), only those from Brazil, Peru, and Poland had MAF >1% and thus could be tested for genetic association.

genome-wide significance previously reported in a large meta-analysis of 12,531 Europeans and 8,216 Asians[37] in our discovery GWAS for PACG. None of the associations (**Supplementary Table 8**) survived correction for multiple comparisons. We note nominal evidence of association with PACG at the *ABCC5* locus, which we previously reported[38] as being associated with anterior chamber depth (for SNP rs4148579, pairwise $r^2 = 0.99$ with the previously reported rs1401999; OR = 1.07, $P = 0.017$).

We then checked whether any of the five newly associated PACG loci directly underlie functional genomic elements. We observed that almost all of the sentinel SNPs as well as SNPs in linkage disequilibrium (LD) are located within potential transcription factor binding sites (**Supplementary Table 9**)[39–41]. None of the sentinel SNPs tag ($r^2 > 0.8$) any exonic SNPs in genes within the respective loci. Examination of recently available large-scale expression quantitative trait locus (eQTL) mapping databases[42,43] indicated that only SNPs rs3739821 on chromosome 9 and rs7494379 on chromosome 14 are significant eQTLs in human tissues (**Supplementary Table 10**). However, the data may allow us to draw limited inferences, as rs3739821 has significant eQTL effects on *DPM2* ($P = 1.44 \times 10^{-12}$) and *FAM102A* ($P = 4.57 \times 10^{-6}$), as well as on the neighboring *ST6GALNAC6* ($P = 6.79 \times 10^{-20}$) and *ST6GALNAC4* ($P = 5.32 \times 10^{-6}$) genes[42]. Looking up our loci in a second eQTL database derived from gene expression analysis in blood cells[44], SNP rs3739821 has a significant

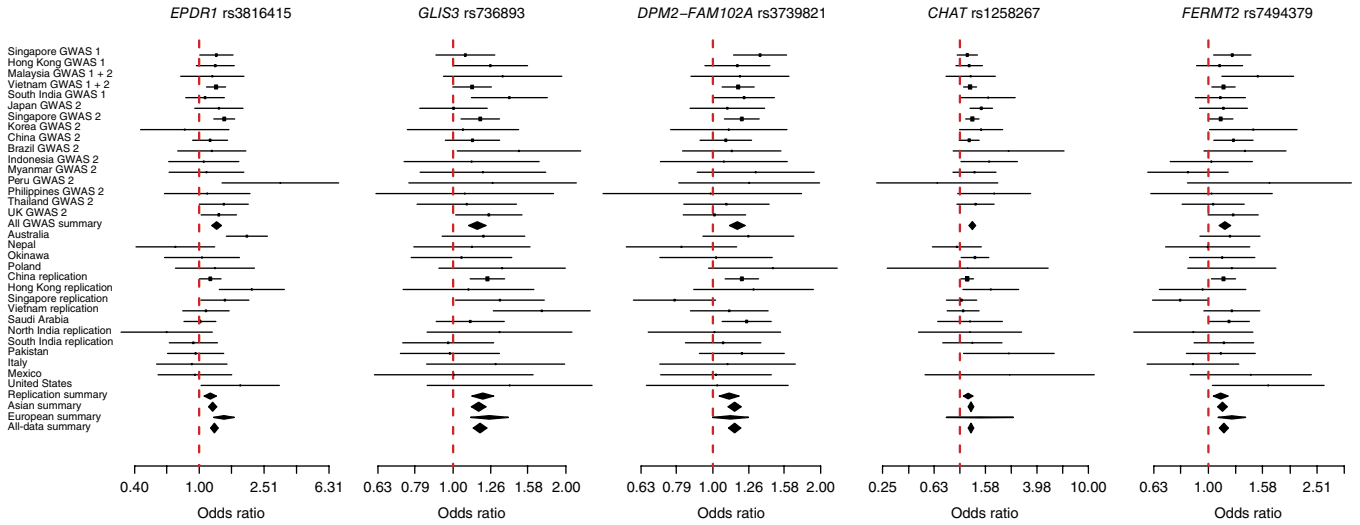

Figure 3 Forest plots for the five new genome-wide significant loci. Point estimates for each locus are denoted as risk allele odds ratios, accompanied by horizontal lines representing the 95% confidence interval for each point estimate. Diamonds represent meta-analyses for the GWAS discovery stage, replication stage, all Asians, and all Europeans, as well as for all samples. The vertical dashed red line represents an OR of 1.00, indicating no effect.

eQTL effect on *ST6GALNAC4* in monocytes, associated with lower expression ($\beta = -0.1$, $P = 2.4 \times 10^{-8}$). Further work is needed to determine the functional effects of these variants on PACG susceptibility.

In summary, our expanded GWAS and replication study of PACG has identified five new susceptibility loci, thus bringing the total number of replicated loci to eight. These eight loci explain up to 1.8% of the overall disease variance in PACG, in line with observations for many complex diseases[45,46]. These results further reinforce the potential importance of cell–cell adhesion and collagen metabolism in PACG pathogenesis. Furthermore, our observations newly implicate acetylcholine metabolism, yet uncharacterized metabolic pathways mediated through zinc-finger activation and repression of transcription, and changes in glycosylation as candidate pathways for future work aimed at identifying the mechanisms responsible for PACG susceptibility.

URLs. PLINK, http://pngu.mgh.harvard.edu/~purcell/plink/; R statistical package, https://www.r-project.org/; IMPUTE, https://mathgen.stats.ox.ac.uk/impute/impute_v2.html.

METHODS

Methods and any associated references are available in the online version of the paper.

Accession codes. The genome-wide association summary statistics for all SNP markers with direct microarray genotyping together with imputation fine-mapping of the significant loci are provided as the **Supplementary Data Set**.

Note: Any Supplementary Information and Source Data files are available in the online version of the paper.

ACKNOWLEDGMENTS

This research is supported by the Singapore Ministry of Health's National Medical Research Council under its Translational and Clinical Research (TCR) Flagship Programme Grant Stratified Medicine for Primary Angle Closure Glaucoma (NMRC/TCR/008-SERI/2013) and the Singapore Translational Research (STaR) Investigator Award Singapore Angle Closure Glaucoma Program Characterization, Prevention, and Management (NMRC/STAR/0023/2014), as well as the Biomedical Research Council, Agency for Science, Technology and Research (A-STAR), Singapore. A.T.L.-S. gratefully acknowledges support from grants RUI 1001/PPSP/812101 and RUI 1001/PPSP/812152 from the Universiti Sains Malaysia. H.J., C.Q., and N. Wang acknowledge support from the Program of Beijing Scholars (2013), Leading Talents–High-Level Talents of the Health System of Beijing (2009-1-05), and the National Major Scientific and Technological Special Project for 'Significant New Drugs Development' (2011ZX09302-007-05), as well as Project of the National Natural Science Foundation of China (81570837) grants.

AUTHOR CONTRIBUTIONS

T.A. and C.C. Khor conceived the project. T. Do., H.J., M.N., R.G., K.A.-A., R. Duvesh., L.J.C., Z.L., M.E.N., S.A.P., C.Q., H.-T.W., H. Sakai., M.B.d.M., Y.A., T.L.H.D., Y.I., R.A.P.-G., T.Z., A.C.D., J.B.J., P.O.S.T., T.A.T., H.A., F.A., S.M., P.T.K.C., L.A.A., T. Dada., T.T.L., M.S.A., N.K., B.W., Y.Y.A., J.M.-N., S.V., S.S., R.H., A.J., M.B., D.G., D.H.S., H.W., V.K.Y., L.W.Y., T.B.T., M.M., T.T.N., E.U.L., K.-H.P., W.A.W., R.S.K., C.T., Y.K., S.S.T., K.P., J.F.S., Y.H.S., A.F., M.O., J.S.M.L., V.T., C.C. Khaing., T.M., S.N., C.-Y.K., G.T., S.F., R.W., H.M., T.T.G.N., T.D.T., M.U., J.M.M., N.R., Y.M.A., R.D.R., S.A.V., S.K.F., Z.X., X.Y.C., J.N.F., K.S.S., T.T.W., D.T.Q., R.V., S. Kavitha., S.R.K., N. Soumittra., B.S., B.-A.L., J.O., J.P.C.d.V., V.P.C., R.Y.A., B.B.d.S., C.C.S., M.C.A., E.K.-J., G.B.F., V.C.T., R.F., Y.J., N. Waseem., S.L., H.N.P., S.A.-S., E.R.C., M.I.K., R. Dada., K. Mohanty., M.A.F., A.W.H., K.P.B., E.H.G., A.P., T.P., M.A.T.C., I.R.F., C.S.L., E.R., V.W.I., G.C., G.P., C.L., P.R., L.M., S.C., J.C.H.C., B.N.K.C., J.W.H.S., H.M.T., K.T.O., A.T.H., V.H.Y., X.-Y.N., F.P., D.P., P.F., J.J.W., P.M., J.H.F., R.R.A., M.A.H., R. Stead., R. Quino., S.N.Z., U.L., R. Shetty., M.Z., H.W.B., N.L.O., T.K., A.M., W.L.H., L.D., Y.H.H., C.A.K., M.K., Z.E.D., J.I.M.P., A.G., J.W.J., T.S.H., N. Srisamran, T.S., S.H.S., V.H.D., S.S.B., C.-L.H., D.T.T., R. Sihota., S.-C.L., K. Mori., S. Kinoshita., A.I.d.H., R. Qamar., Y.-X.W., Y.Y.T., E.-S.T., C.H.-M., D.L.-G., S.M.S., C.-Y.C., J.C.Z., C.P.P., H.T.T.B., O.H., J.E.C., D.P.E., M.Y., J.M.N., M.L.G.-F., L.X., R.R., A.T.L.-S., T.Y.W., S.A.-O., N.H.D., P.S., C.C.T., P.J.F., L.V., K.T., E.N.V., and N. Wang were responsible for sample collection, data analysis, and sample administration. M.L.H., M.S., E.P., S.J.D., N.V.V.C., J.B., Y.X.Z., A.K., S.T.L., S.H.C., R.P.E., A.S., K.H.P., J.A., G.B., H. Snippe., and B.B. contributed control data sets with genome-wide genotyping data. M.-C.L., A.S.C., S.R.G., Y.F.C., and E.N.V. were responsible for molecular biology work and pathological tissue staining and interpretation. The manuscript was written by C.C. Khor, with approval from all authors. All authors read and approved the final version of the manuscript for publication. T.A. was responsible for obtaining financial support for the study.

COMPETING FINANCIAL INTERESTS

The authors declare no competing financial interests.

1. Vithana, E.N. *et al.* Genome-wide association analyses identify three new susceptibility loci for primary angle closure glaucoma. *Nat. Genet.* **44**, 1142–1146 (2012).

2. Thylefors, B., Négrel, A.D., Pararajasegaram, R. & Dadzie, K.Y. Global data on blindness. *Bull. World Health Organ.* **73**, 115–121 (1995).
3. Hysi, P.G. *et al.* Genome-wide analysis of multi-ancestry cohorts identifies new loci influencing intraocular pressure and susceptibility to glaucoma. *Nat. Genet.* **46**, 1126–1130 (2014).
4. Gharahkhani, P. *et al.* Common variants near *ABCA1*, *AFAP1* and *GMDS* confer risk of primary open-angle glaucoma. *Nat. Genet.* **46**, 1120–1125 (2014).
5. Wiggs, J.L. *et al.* Common variants at 9p21 and 8q22 are associated with increased susceptibility to optic nerve degeneration in glaucoma. *PLoS Genet.* **8**, e1002654 (2012).
6. Aung, T. *et al.* A common variant mapping to *CACNA1A* is associated with susceptibility to exfoliation syndrome. *Nat. Genet.* **47**, 387–392 (2015).
7. Foster, P.J., Buhrmann, R., Quigley, H.A. & Johnson, G.J. The definition and classification of glaucoma in prevalence surveys. *Br. J. Ophthalmol.* **86**, 238–242 (2002).
8. Cheng, J.W., Zong, Y., Zeng, Y.Y. & Wei, R.L. The prevalence of primary angle closure glaucoma in adult Asians: a systematic review and meta-analysis. *PLoS One* **9**, e103222 (2014).
9. Quigley, H.A. & Broman, A.T. The number of people with glaucoma worldwide in 2010 and 2020. *Br. J. Ophthalmol.* **90**, 262–267 (2006).
10. Foster, P.J. & Johnson, G.J. Glaucoma in China: how big is the problem? *Br. J. Ophthalmol.* **85**, 1277–1282 (2001).
11. Foster, P.J. *et al.* The prevalence of glaucoma in Chinese residents of Singapore: a cross-sectional population survey of the Tanjong Pagar district. *Arch. Ophthalmol.* **118**, 1105–1111 (2000).
12. Dandona, L. *et al.* Angle-closure glaucoma in an urban population in southern India. The Andhra Pradesh eye disease study. *Ophthalmology* **107**, 1710–1716 (2000).
13. Quigley, H.A., Congdon, N.G. & Friedman, D.S. Glaucoma in China (and worldwide): changes in established thinking will decrease preventable blindness. *Br. J. Ophthalmol.* **85**, 1271–1272 (2001).
14. Purdue, M.P. *et al.* Genome-wide association study of renal cell carcinoma identifies two susceptibility loci on 2p21 and 11q13.3. *Nat. Genet.* **43**, 60–65 (2011).
15. International Parkinson Disease Genomics Consortium. Imputation of sequence variants for identification of genetic risks for Parkinson's disease: a meta-analysis of genome-wide association studies. *Lancet* **377**, 641–649 (2011).
16. Ellinor, P.T. *et al.* Meta-analysis identifies six new susceptibility loci for atrial fibrillation. *Nat. Genet.* **44**, 670–675 (2012).
17. Gudbjartsson, D.F. *et al.* A sequence variant in *ZFHX3* on 16q22 associates with atrial fibrillation and ischemic stroke. *Nat. Genet.* **41**, 876–878 (2009).
18. Pomerantz, M.M. *et al.* The 8q24 cancer risk variant rs6983267 shows long-range interaction with *MYC* in colorectal cancer. *Nat. Genet.* **41**, 882–884 (2009).
19. Tuupanen, S. *et al.* The common colorectal cancer predisposition SNP rs6983267 at chromosome 8q24 confers potential to enhanced Wnt signaling. *Nat. Genet.* **41**, 885–890 (2009).
20. Gregorio-King, C.C. *et al. MERP1*: a mammalian ependymin-related protein gene differentially expressed in hematopoietic cells. *Gene* **286**, 249–257 (2002).
21. Dolmans, G.H. *et al.* Wnt signaling and Dupuytren's disease. *N. Engl. J. Med.* **365**, 307–317 (2011).
22. Barone, R. *et al.* DPM2-CDG: a muscular dystrophy–dystroglycanopathy syndrome with severe epilepsy. *Ann. Neurol.* **72**, 550–558 (2012).
23. Wang, D.Y., Fulthorpe, R., Liss, S.N. & Edwards, E.A. Identification of estrogen-responsive genes by complementary deoxyribonucleic acid microarray and characterization of a novel early estrogen-induced gene: *EEIG1*. *Mol. Endocrinol.* **18**, 402–411 (2004).
24. Shi, L. *et al.* Overexpression of PIP5KL1 suppresses cell proliferation and migration in human gastric cancer cells. *Mol. Biol. Rep.* **37**, 2189–2198 (2010).
25. Lachkar, Y. & Bouassida, W. Drug-induced acute angle closure glaucoma. *Curr. Opin. Ophthalmol.* **18**, 129–133 (2007).
26. Mandak, J.S., Minerva, P., Wilson, T.W. & Smith, E.K. Angle closure glaucoma complicating systemic atropine use in the cardiac catheterization laboratory. *Cathet. Cardiovasc. Diagn.* **39**, 262–264 (1996).
27. Shen, Z. *et al.* Novel focal adhesion protein kindlin-2 promotes the invasion of gastric cancer cells through phosphorylation of integrin β1 and β3. *J. Surg. Oncol.* **108**, 106–112 (2013).
28. Kim, Y.S., Nakanishi, G., Lewandoski, M. & Jetten, A.M. GLIS3, a novel member of the GLIS subfamily of Krüppel-like zinc finger proteins with repressor and activation functions. *Nucleic Acids Res.* **31**, 5513–5525 (2003).
29. Senée, V. *et al.* Mutations in *GLIS3* are responsible for a rare syndrome with neonatal diabetes mellitus and congenital hypothyroidism. *Nat. Genet.* **38**, 682–687 (2006).
30. Barrett, J.C. *et al.* Genome-wide association study and meta-analysis find that over 40 loci affect risk of type 1 diabetes. *Nat. Genet.* **41**, 703–707 (2009).
31. Cho, Y.S. *et al.* Meta-analysis of genome-wide association studies identifies eight new loci for type 2 diabetes in east Asians. *Nat. Genet.* **44**, 67–72 (2012).
32. Dupuis, J. *et al.* New genetic loci implicated in fasting glucose homeostasis and their impact on type 2 diabetes risk. *Nat. Genet.* **42**, 105–116 (2010).
33. Burdon, K.P. *et al.* Genome-wide association study identifies susceptibility loci for open angle glaucoma at *TMCO1* and *CDKN2B-AS1*. *Nat. Genet.* **43**, 574–578 (2011).
34. Chen, Y. *et al.* Common variants near *ABCA1* and in *PMM2* are associated with primary open-angle glaucoma. *Nat. Genet.* **46**, 1115–1119 (2014).
35. Li, Z. *et al.* A common variant near *TGFBR3* is associated with primary open angle glaucoma. *Hum. Mol. Genet.* **24**, 3880–3892 (2015).
36. Nongpiur, M.E. *et al.* Lack of association between primary angle-closure glaucoma susceptibility loci and the ocular biometric parameters anterior chamber depth and axial length. *Invest. Ophthalmol. Vis. Sci.* **54**, 5824–5828 (2013).
37. Cheng, C.Y. *et al.* Nine loci for ocular axial length identified through genome-wide association studies, including shared loci with refractive error. *Am. J. Hum. Genet.* **93**, 264–277 (2013).
38. Nongpiur, M.E. *et al. ABCC5*, a gene that influences the anterior chamber depth, is associated with primary angle closure glaucoma. *PLoS Genet.* **10**, e1004089 (2014).
39. Boyle, A.P. *et al.* Annotation of functional variation in personal genomes using RegulomeDB. *Genome Res.* **22**, 1790–1797 (2012).
40. Ward, L.D. & Kellis, M. HaploReg: a resource for exploring chromatin states, conservation, and regulatory motif alterations within sets of genetically linked variants. *Nucleic Acids Res.* **40**, D930–D934 (2012).
41. ENCODE Project Consortium. An integrated encyclopedia of DNA elements in the human genome. *Nature* **489**, 57–74 (2012).
42. Westra, H.J. *et al.* Systematic identification of *trans* eQTLs as putative drivers of known disease associations. *Nat. Genet.* **45**, 1238–1243 (2013).
43. GTEx Consortium. The Genotype-Tissue Expression (GTEx) project. *Nat. Genet.* **45**, 580–585 (2013).
44. Fairfax, B.P. *et al.* Genetics of gene expression in primary immune cells identifies cell type–specific master regulators and roles of HLA alleles. *Nat. Genet.* **44**, 502–510 (2012).
45. Okada, Y. *et al.* Genetics of rheumatoid arthritis contributes to biology and drug discovery. *Nature* **506**, 376–381 (2014).
46. Speliotes, E.K. *et al.* Association analyses of 249,796 individuals reveal 18 new loci associated with body mass index. *Nat. Genet.* **42**, 937–948 (2010).

Chiea Chuen Khor[1–3,124], Tan Do[4,124], Hongyan Jia[5,124], Masakazu Nakano[6,124], Ronnie George[7,124], Khaled Abu-Amero[8,9,124], Roopam Duvesh[10,124], Li Jia Chen[11,124], Zheng Li[1], Monisha E Nongpiur[2], Shamira A Perera[2], Chunyan Qiao[5], Hon-Tym Wong[12], Hiroshi Sakai[13], Mônica Barbosa de Melo[14], Mei-Chin Lee[2], Anita S Chan[2], Yaakub Azhany[15], Thi Lam Huong Dao[4], Yoko Ikeda[16], Rodolfo A Perez-Grossmann[17], Tomasz Zarnowski[18], Alexander C Day[19–21], Jost B Jonas[22], Pancy O S Tam[11], Tuan Anh Tran[23], Humaira Ayub[24], Farah Akhtar[25], Shazia Micheal[26], Paul T K Chew[27], Leyla A Aljasim[28], Tanuj Dada[29], Tam Thi Luu[30], Mona S Awadalla[31], Naris Kitnarong[32], Boonsong Wanichwecharungruang[33,34], Yee Yee Aung[35], Jelinar Mohamed-Noor[36], Saravanan Vijayan[10], Sripriya Sarangapani[37], Rahat Husain[2,38], Aliza Jap[2,38], Mani Baskaran[2], David Goh[2], Daniel H Su[2], Huaizhou Wang[5], Vernon K Yong[12], Leonard W Yip[12], Tuyet Bach Trinh[23], Manchima Makornwattana[39], Thanh Thu Nguyen[40], Edgar U Leuenberger[41,42], Ki-Ho Park[43], Widya Artini Wiyogo[44,45], Rajesh S Kumar[46], Celso Tello[47], Yasuo Kurimoto[48], Suman S Thapa[49], Kessara Pathanapitoon[50], John F Salmon[51], Yong Ho Sohn[52], Antonio Fea[53], Mineo Ozaki[54,55], Jimmy S M Lai[56], Visanee Tantisevi[57], Chaw Chaw Khaing[58], Takanori Mizoguchi[59], Satoko Nakano[60], Chan-Yun Kim[61], Guangxian Tang[62], Sujie Fan[63], Renyi Wu[64], Hailin Meng[65], Thi Thuy Giang Nguyen[4], Tien Dat Tran[4], Morio Ueno[16], Jose Maria Martinez[66], Norlina Ramli[67,68], Yin Mon Aung[69,70], Rigo Daniel Reyes[71,72],

Stephen A Vernon[73,74], Seng Kheong Fang[75], Zhicheng Xie[1], Xiao Yin Chen[1], Jia Nee Foo[1], Kar Seng Sim[1], Tina T Wong[2], Desmond T Quek[2], Rengaraj Venkatesh[76], Srinivasan Kavitha[76], Subbiah R Krishnadas[77], Nagaswamy Soumittra[37], Balekudaru Shantha[7], Boon-Ang Lim[12], Jeanne Ogle[12], José P C de Vasconcellos[78], Vital P Costa[77], Ricardo Y Abe[77], Bruno B de Souza[14], Chelvin C Sng[27], Maria C Aquino[27], Ewa Kosior-Jarecka[18], Guillermo Barreto Fong[79], Vania Castro Tamanaja[80], Ricardo Fujita[81], Yuzhen Jiang[19–21], Naushin Waseem[19,21], Sancy Low[19–21], Huan Nguyen Pham[23], Sami Al-Shahwan[28], E Randy Craven[28,82], Muhammad Imran Khan[83], Rrima Dada[29], Kuldeep Mohanty[29], Muneeb A Faiq[29], Alex W Hewitt[84,85], Kathryn P Burdon[31,84], Eng Hui Gan[36], Anuwat Prutthipongsit[39], Thipnapa Patthanathamrongkasem[39], Mary Ann T Catacutan[41], Irene R Felarca[41], Chona S Liao[41], Emma Rusmayani[44], Vira Wardhana Istiantoro[44], Giulia Consolandi[53], Giulia Pignata[53], Carlo Lavia[53], Prin Rojanapongpun[57], Lerprat Mangkornkanokpong[86], Sunee Chansangpetch[86], Jonathan C H Chan[87], Bonnie N K Choy[56], Jennifer W H Shum[56], Hlaing May Than[88], Khin Thida Oo[69,70], Aye Thi Han[69,70], Victor H Yong[2], Xiao-Yu Ng[2], Shuang Ru Goh[2], Yaan Fun Chong[2], Martin L Hibberd[1], Mark Seielstad[89], Eileen Png[1], Sarah J Dunstan[90,91], Nguyen Van Vinh Chau[92], Jinxin Bei[93,94], Yi Xin Zeng[93–95], Abhilasha Karkey[96], Buddha Basnyat[96], Francesca Pasutto[97], Daniela Paoli[98], Paolo Frezzotti[99], Jie Jin Wang[100], Paul Mitchell[100], John H Fingert[101,102], R Rand Allingham[2,103], Michael A Hauser[2,103,104], Soon Thye Lim[105], Soo Hong Chew[106], Richard P Ebstein[107], Anavaj Sakuntabhai[108,109], Kyu Hyung Park[110], Jeeyun Ahn[111], Greet Boland[112], Harm Snippe[112], Richard Stead[73], Raquel Quino[71], Su Nyunt Zaw[69,70], Urszula Lukasik[18], Rohit Shetty[46], Mimiwati Zahari[67,68], Hyoung Won Bae[61], Nay Lin Oo[58], Toshiaki Kubota[60], Anita Manassakorn[57], Wing Lau Ho[86], Laura Dallorto[53], Young Hoon Hwang[52], Christine A Kiire[51], Masako Kuroda[48], Zeiras Eka Djamal[44], Jovell Ian M Peregrino[41], Arkasubhra Ghosh[46,113], Jin Wook Jeoung[43], Tung S Hoan[40], Nuttamon Srisamran[39], Thayanithi Sandragasu[36], Saw Htoo Set[35], Vi Huyen Doan[30], Shomi S Bhattacharya[21], Ching-Lin Ho[2], Donald T Tan[2], Ramanjit Sihota[29], Seng-Chee Loon[27], Kazuhiko Mori[16], Shigeru Kinoshita[16], Anneke I den Hollander[26,83], Raheel Qamar[24,114], Ya-Xing Wang[115], Yik Y Teo[1,116–119], E-Shyong Tai[116,120], Curt Hartleben-Matkin[121], David Lozano-Giral[122], Seang Mei Saw[2,116], Ching-Yu Cheng[2,27], Juan C Zenteno[122,123], Chi Pui Pang[11], Huong T T Bui[23], Owen Hee[12], Jamie E Craig[31], Deepak P Edward[28,82], Michiko Yonahara[13], Jamil Miguel Neto[78], Maria L Guevara-Fujita[81], Liang Xu[115], Robert Ritch[47], Ahmad Tajudin Liza-Sharmini[15], Tien Y Wong[2], Saleh Al-Obeidan[8], Nhu Hon Do[4,125], Periasamy Sundaresan[10,125], Clement C Tham[11,125], Paul J Foster[19–21,125], Lingam Vijaya[2,7,125], Kei Tashiro[6,125], Eranga N Vithana[2,125], Ningli Wang[5,115,125] & Tin Aung[2,27,125]

[1]Genome Institute of Singapore, A-STAR, Singapore. [2]Singapore Eye Research Institute, Singapore National Eye Centre and Eye ACP, Duke–National University of Singapore, Singapore. [3]Department of Biochemistry, National University of Singapore, Singapore. [4]Vietnam National Institute of Ophthalmology, Hanoi, Vietnam. [5]Beijing Tongren Eye Center, Beijing Tongren Hospital, Capital Medical University, Beijing Ophthalmology and Visual Science Key Laboratory, Beijing, China. [6]Department of Genomic Medical Sciences, Kyoto Prefectural University of Medicine, Kyoto, Japan. [7]Jadhavbhai Nathamal Singhvi Department of Glaucoma, Medical Research Foundation, Sankara Nethralaya, Chennai, India. [8]Department of Ophthalmology, College of Medicine, King Saud University, Riyadh, Saudi Arabia. [9]Department of Ophthalmology, College of Medicine, University of Florida, Jacksonville, Florida, USA. [10]Department of Genetics, Aravind Medical Research Foundation, Madurai, India. [11]Department of Ophthalmology and Visual Sciences, Chinese University of Hong Kong, Hong Kong, China. [12]Department of Ophthalmology, Tan Tock Seng Hospital, NHG Eye Institute, Singapore. [13]Department of Ophthalmology, University of the Ryukyus, Okinawa, Nishihara, Japan. [14]Center of Molecular Biology and Genetic Engineering, University of Campinas, Campinas, Brazil. [15]Department of Ophthalmology, School of Medical Sciences, Health Campus, Universiti Sains Malaysia and Hospital Universiti Sains Malaysia, Kelantan, Malaysia. [16]Department of Ophthalmology, Kyoto Prefectural University of Medicine, Kyoto, Japan. [17]Instituto de Glaucoma y Catarata, Lima, Peru. [18]Department of Diagnostics and Microsurgery of Glaucoma, Medical University, Lublin, Poland. [19]NIHR Biomedical Research Centre for Ophthalmology at Moorfields Eye Hospital and University College London Institute of Ophthalmology, London, UK. [20]Glaucoma Service, Moorfields Eye Hospital NHS Foundation Trust, London, UK. [21]Division of Genetics, UCL Institute of Ophthalmology, London, UK. [22]Department of Ophthalmology, Medical Faculty Mannheim of the Ruprecht Karls University Heidelberg, Heidelberg, Germany. [23]Ho Chi Minh City Eye Hospital, Ho Chi Minh City, Vietnam. [24]Department of Biosciences, COMSATS Institute of Information Technology, Islamabad, Pakistan. [25]Pakistan Institute of Ophthalmology, Al-Shifa Trust Eye Hospital, Rawalpindi, Pakistan. [26]Department of Ophthalmology, Radboud University Medical Centre, Nijmegen, the Netherlands. [27]Department of Ophthalmology, National University Health System, Yong Loo Lin School of Medicine, National University of Singapore, Singapore. [28]King Khaled Eye Specialist Hospital, Riyadh, Saudi Arabia. [29]All India Institute of Medical Sciences, New Delhi, India. [30]Department of Glaucoma, Da Nang Eye Hospital, Da Nang City, Vietnam. [31]Department of Ophthalmology, Flinders University, Flinders Medical Centre, Adelaide, South Australia, Australia. [32]Department of Ophthalmology, Faculty of Medicine Siriraj Hospital, Mahidol University, Bangkok, Thailand. [33]Glaucoma Services, Department of Ophthalmology, Rajavithi Hospital, Bangkok, Thailand. [34]College of Medicine, Rangsit University, Bangkok, Thailand. [35]Mandalay Eye Department, Mandalay Eye ENT Hospital, University of Medicine Mandalay, Mandalay, Myanmar. [36]Department of Ophthalmology, Hospital Kuala Lumpur, Kuala Lumpur, Malaysia. [37]Vision Research Foundation, Sankara Nethralaya, Chennai, India. [38]Division of Ophthalmology, Changi General Hospital, Singapore. [39]Department of Ophthalmology, Thammasat University Faculty of Medicine, Rangsit, Thailand. [40]Eye Department, Viet Tiep General Hospital, Hai Phong, Vietnam. [41]Asian Eye Institute, Manila, Philippines. [42]Division of Ophthalmology, University of the East, Manila, Philippines. [43]Department of Ophthalmology, Seoul National University College of Medicine, Seoul, Republic of Korea. [44]Glaucoma Service Jakarta Eye Center, Jakarta, Indonesia. [45]Faculty of Medicine, University of Indonesia, Jakarta, Indonesia. [46]Narayana Nethralaya Eye Hospital, Bangalore, India. [47]Einhorn Clinical Research Center, New York Eye and Ear Infirmary of Mount Sinai, New York, New York, USA. [48]Department of Ophthalmology, Kobe City Medical Center General Hospital, Kobe, Japan. [49]Nepal Glaucoma Eye Clinic, Tilganga Institute of Ophthalmology, Kathmandu, Nepal. [50]Department of Ophthalmology, Faculty of Medicine, Chiang Mai University, Chiang Mai, Thailand. [51]Oxford Eye Hospital, John Radcliffe Hospital, Oxford University Hospitals NHS Trust, Oxford, UK. [52]Department of Ophthalmology, Konyang University, Kim's Eye Hospital, Myung-Gok Eye Research Institute, Seoul, Republic of Korea. [53]Dipartimento di Scienze

Chirurgiche, Università di Torino, Turin, Italy. [54]Ozaki Eye Hospital, Hyuga, Japan. [55]Department of Ophthalmology, Faculty of Medicine, University of Miyazaki, Miyazaki, Japan. [56]Department of Ophthalmology, University of Hong Kong, Hong Kong, China. [57]Department of Ophthalmology, Faculty of Medicine, Chulalongkorn University, Bangkok, Thailand. [58]Department of Ophthalmology, No. 1 Defence Services General Hospital, Yangon, Myanmar. [59]Mizoguchi Eye Hospital, Sasebo, Japan. [60]Department of Ophthalmology, Oita University Faculty of Medicine, Oita, Japan. [61]Department of Ophthalmology, Yonsei University College of Medicine, Seoul, Republic of Korea. [62]Shijiazhuang First Eye Hospital, Shijiazhuang, China. [63]Handan Eye Hospital, Handan, China. [64]Eye Institute and Affiliated Xiamen Eye Center, Xiamen University, Fujian Provincial Key Laboratory of Ophthalmology and Visual Science, Xiamen, China. [65]Anyang Eye Hospital, Anyang, China. [66]Department of Ophthalmology, Pasig City General Hospital, Pasig City, Philippines. [67]University of Malaya, Eye Research Centre, Kuala Lumpur, Malaysia. [68]Department of Ophthalmology, Faculty of Medicine, University of Malaya, Kuala Lumpur, Malaysia. [69]Myanmar Eye Centre, Pun Hlaing Silom Hospital, Yangon, Myanmar. [70]Myanmar Eye Centre, Shwe La Min Hospital, Yangon, Myanmar. [71]Department of Ophthalmology/Glaucoma Section, Asian Hospital and Medical Center, Muntinlupa City, Philippines. [72]Binan Doctors Eye Center, Binan Doctors Hospital, Laguna, Philippines. [73]Department of Ophthalmology, University Hospital Nottingham, University of Nottingham, Nottingham, UK. [74]BMI Park Hospital Nottingham, Nottingham, UK. [75]International Specialist Eye Centre, Kuala Lumpur, Malaysia. [76]Glaucoma Clinic, Aravind Eye Hospital, Pondicherry, India. [77]Glaucoma Clinic, Aravind Eye Hospital, Madurai, India. [78]Department of Ophthalmology, Faculty of Medical Sciences, University of Campinas, Campinas, Brazil. [79]Instituto de Ciencias Médicas, Lima, Peru. [80]Hospital Nacional Arzobispo Loayza, Lima, Peru. [81]Centro de Genética y Biología Molecular, Universidad de San Martín de Porres, Lima, Peru. [82]Wilmer Eye Institute, Johns Hopkins Hospital School of Medicine, Baltimore, Maryland, USA. [83]Department of Human Genetics, Radboud University Medical Centre, Nijmegen, the Netherlands. [84]Menzies Institute for Medical Research, University of Tasmania, Hobart, Tasmania, Australia. [85]Centre for Eye Research Australia, University of Melbourne, Royal Victorian Eye and Ear Hospital, Melbourne, Victoria, Australia. [86]Department of Ophthalmology, King Chulalongkorn Memorial Hospital, Bangkok, Thailand. [87]Department of Ophthalmology, Queen Mary Hospital, Hong Kong, China. [88]Department of Ophthalmology, North Okkalarpa General Hospital, Yangon, Myanmar. [89]Institute for Human Genetics, University of California, San Francisco, San Francisco, California, USA. [90]Oxford University Clinical Research Unit, Ho Chi Minh City, Vietnam. [91]Peter Doherty Institute for Infection and Immunity, University of Melbourne, Melbourne, Victoria, Australia. [92]Hospital for Tropical Diseases, Ho Chi Minh City, Vietnam. [93]Sun Yat-Sen University Cancer Center, State Key Laboratory of Oncology in South China, Collaborative Innovation Center for Cancer Medicine, Guangzhou, China. [94]Department of Experimental Research, Sun Yat-sen University Cancer Center, Guangzhou, China. [95]Peking Union Medical College, Beijing, China. [96]Oxford University Clinical Research Unit–Nepal, Patan Academy of Health Sciences, Patan Hospital, Patan, Nepal. [97]Institute of Human Genetics, Friedrich Alexander Universität Erlangen-Nürnberg (FAU), Erlangen, Germany. [98]Department of Ophthalmology, Monfalcone Hospital, Gorizia, Italy. [99]Department of Surgery, Section of Ophthalmology, University of Siena, Siena, Italy. [100]Centre for Vision Research, Department of Ophthalmology, Westmead Institute for Medical Research, University of Sydney, Sydney, New South Wales, Australia. [101]Department of Ophthalmology and Visual Sciences, Carver College of Medicine, University of Iowa, Iowa City, Iowa, USA. [102]Wynn Institute for Vision Research, University of Iowa, Iowa City, Iowa, USA. [103]Department of Ophthalmology, Duke University Eye Center, Durham, North Carolina, USA. [104]Department of Medicine, Duke University Medical Center, Durham, North Carolina, USA. [105]Division of Medical Oncology, National Cancer Centre, Singapore. [106]Department of Economics, National University of Singapore, Singapore. [107]Department of Psychology, National University of Singapore, Singapore. [108]Institut Pasteur, Functional Genetics of Infectious Diseases Unit, Department of Genomes and Genetics, Paris, France. [109]Centre National de la Recherche Scientifique, Unité de Recherche Associée 3012, Paris, France. [110]Department of Ophthalmology, Seoul National University Bundang Hospital, Gyeonggi, Republic of Korea. [111]Department of Ophthalmology, Seoul Metropolitan Government Seoul National University Boramae Medical Center, Seoul, Republic of Korea. [112]Department of Medical Microbiology and Virology, University Medical Center Utrecht, Utrecht, the Netherlands. [113]GROW Research Laboratory, Narayana Nethralaya Foundation, Bangalore, India. [114]Department of Biochemistry, Al-Nafees Medical College and Hospital, Isra University, Islamabad, Pakistan. [115]Beijing Institute of Ophthalmology, Beijing Tongren Hospital, Capital Medical University, Beijing, China. [116]Saw Swee Hock School of Public Health, National University of Singapore, Singapore. [117]Life Sciences Institute, National University of Singapore, Singapore. [118]National University of Singapore Graduate School for Integrative Science and Engineering, National University of Singapore, Singapore. [119]Department of Statistics and Applied Probability, National University of Singapore, Singapore. [120]Department of Medicine, Yong Loo Lin School of Medicine, National University of Singapore, Singapore. [121]Department of Glaucoma, Institute of Ophthalmology 'Conde de Valenciana', Mexico City, Mexico. [122]Department of Genetics, Institute of Ophthalmology 'Conde de Valenciana', Mexico City, Mexico. [123]Department of Biochemistry, Faculty of Medicine, Universidad Nacional Autónoma de México, Mexico City, Mexico. [124]These authors contributed equally to this work. [125]These authors jointly directed this work. Correspondence should be addressed to C.C. Khor (khorcc@gis.a-star.edu.sg), N. Wang (wningli@vip.163.com) or T.A. (aung_tin@yahoo.co.uk).

ONLINE METHODS

Patient collections. DNA samples from all PACG cases and controls were collected after written informed consent was obtained from each participant, strictly in accordance with the tenets of the Declaration of Helsinki. Details for each case–control collection are provided in the **Supplementary Note**.

Genotyping. For the GWAS discovery stage, genome-wide genotyping was performed using the Illumina 610K/660W and OmniExpress BeadChips following the manufacturer's instructions and as previously described[1].

For the replication stage, the most significantly associated SNPs from the discovery stage were genotyped using Applied Biosystems TaqMan genotyping assays as well as the Sequenom MassARRAY system, as previously described[47]. We performed cross-platform concordance checks and verified > 99.9% concordance of genotypes for the SNP markers surpassing genome-wide significance reported here.

Statistical analysis. Stringent quality checks were performed on a per-SNP and per-sample basis, with removal of SNPs showing a genotyping success rate of <95% or a MAF of <1%, as well as deviation from Hardy–Weinberg equilibrium ($P < 1 \times 10^{-6}$ for deviation). Samples were similarly checked, and those with a genotyping success rate of <95% were removed, as were those showing excesses heterozygosity and outliers on principal-component analysis of genetic ancestry. PACG cases were contrasted to ancestry- and geographically matched controls for each country strata, as is now routinely done in GWAS[48–50]. PACG cases and controls appeared to be well matched in terms of ancestry for each stratum, as well as in overall assessment (**Fig. 1** and **Supplementary Figs. 10** and **11**). In the discovery stage, we analyzed a total of 745,080 SNPs with direct genotyping and > 4,500,000 SNPs with imputation. The relationship between each variable genetic SNP marker and PACG disease was measured using logistic regression with further adjustments for principal components of genetic stratification. We observed minimal overall genomic inflation in each of the discovery sample collections and in the discovery meta-analysis (overall λ_{GC} for the meta-analysis = 1.05; **Supplementary Fig. 12** and **Supplementary Table 1**). We then performed a meta-analysis of all the discovery-stage PACG collections, summarizing the data across the 16 case–control strata (**Supplementary Table 1**) using random-effects meta-analysis. We used the random-effects model to provide for more robust estimation of *P* values and odds ratios in the discovery stage because of the ancestrally and geographically diverse patient collections. Such an approach allows us the best chance of identifying PACG susceptibility variants shared by most of the ancestry groups.

The biological relationships of all remaining samples were then verified using the principle of variability in allele sharing. Identity-by-state information from comparisons of each sample pair was derived using PLINK software (see URLs). For each pair of individuals showing evidence of cryptic relatedness (possibly due either to inadvertent sample duplication or biologically related samples), we excluded the sample with the lower call rate from further analysis. Principal-component analysis was then undertaken to minimize spurious associations due to ancestry differences between PACG cases and controls. Plots of principal components were generated using the R statistical package (see URLs).

For both the GWAS discovery and replication stages, the association between SNP genotypes and PACG disease status was measured using score-based tests (1 degree of freedom). These general tests model additive effects of the minor allele on disease risk. They do not assume any mode of inheritance and are well described elsewhere. Each SNP genotype is coded according to allele dosage: 0 for individuals with the wild-type genotype for a given SNP, 1 for individuals heterozygous for the alternate allele, and 2 for individuals homozygous for the alternate allele.

In the GWAS discovery stage, the association analysis was also adjusted for the principal components of genetic stratification for sample collections where residual population stratification existed. Details on the overall genomic inflation factor and number of principal components used for adjustment in each of the GWAS discovery collections are provided in **Supplementary Table 1**. The genome-wide association summary statistics for all SNP markers with direct microarray genotyping together with imputation fine-mapping of the significant loci are provided as the **Supplementary Data Set**.

As the replication stage only tested a limited number of SNP markers, we were unable to adjust for population stratification in this stage. Nonetheless, association tests were performed for each stratum separately, and the cohorts were subsequently combined in meta-analysis. Meta-analysis was conducted using inverse-variance weights for each PACG case–control collection, which calculates an overall *z* statistic, its corresponding *P* value, and accompanying odds ratios for each SNP analyzed. All *P* values reported here are two-tailed.

At each locus, the sentinel SNP is defined as the most significant directly genotyped SNP within that locus. Independent loci are defined as loci with no LD between them (pairwise r^2 <0.01) and are located more than 1 Mb apart from one another.

Genotype imputation. To improve the genetic resolution beyond that provided by the directly genotyped SNPs present on standard-content GWAS arrays, we performed imputation for the GWAS discovery sample collections using samples and SNP markers passing standard GWAS quality control checks. The imputation and phasing of genotypes were carried out using IMPUTE2 software (see URLs) with a reference panel constructed from cosmopolitan population haplotypes based on data obtained for 2,535 individuals from 26 distinct populations around the world. These data are part of the 1000 Genomes Project Phase 3 (June 2014) release. Imputed genotypes were called with an IMPUTE probability threshold of 0.90, with all other genotypes classified as missing. We applied additional quality control filters to exclude SNP markers with a call rate of <99% should the SNP have a MAF of <5% in either cases or controls. For common SNPs with MAF > 5%, the filtering criterion was set to exclude SNPs with a call rate of <95%.

Power calculation. All statistical power calculations were performed as previously described for two-stage GWAS and replication studies[50]. We present these power calculations for each of the following conditions: (i) GWAS discovery stage only and (ii) GWAS discovery and replication stages (**Supplementary Table 4**).

Expression analysis. Expression of *EPDR1*, *GLIS3*, *DPM2*, *FAM102A*, *PIP5KL1*, and *FERMT2* was assessed by semiquantitative RT–PCR using gene-specific primers (**Supplementary Table 11**) on the following human ocular tissues: sclera, cornea, lens with lens capsule, iris, trabecular meshwork, ciliary body, retina, choroid, optic nerve head, and optic nerve. Human donor eyes were obtained from the Florida Lions Eye Banks and dissected into respective ocular regions for RNA extraction and semiquantitative RT–PCR expression analysis. Ethical approval for this section of the study was granted by the Institutional Review Board of the Singapore Eye Research Institute for donor eyes procured from the Florida Lions Eye Bank. All of the investigated genes produced multiple transcripts through alternative splicing that resulted in several protein isoforms. In this study, we investigated the mRNA expression of the full-length or leading transcript that produced the 'canonical' protein isoform (**Supplementary Table 11**). The NCBI reference sequence from which the primer sequences were derived is indicated for each gene. Primers were selected specifically to target the mRNA and not the genomic DNA of the genes examined. All gene-specific primers therefore spanned an intron, and the sizes of the PCR products obtained (*EPDR1*, 210 bp; *GLIS3*, 247 bp; *DPM2*, 218 bp; *FAM102A*, 155 bp; *PIP5KL1*, 189 bp; *FERMT2*, 159 bp) confirmed the amplification of mRNA. We were unable to successfully amplify a specific PCR product for the *CHAT* gene despite multiple attempts. The ocular expression of CHAT protein was therefore investigated through immunoblot and immunohistochemistry analyses in ocular tissues. Total RNA was extracted from a variety of ocular tissues (sclera, cornea, iris, trabecular meshwork, ciliary body, lens and capsule, retina, choroid, optic nerve head, and optic nerve) with TRIzol reagent (Invitrogen) in accordance with the manufacturer's protocol. First-strand cDNA synthesis was performed with the SuperScript First-Strand Synthesis System for RT–PCR (Invitrogen) using random primers. Semiquantitative RT–PCR was performed according to the manufacturer's protocol, with SYBR Green Mastermix (Invitrogen) using the specified gene primers and equal amounts of cDNA template. The resulting PCR products were separated on a 2%

agarose gel and visualized by ethidium bromide staining. The ubiquitously expressed β-actin (*ACTB*) gene (primers listed in **Supplementary Table 11**) was used as an amplification and normalizing control. All RT–PCR products were resequenced to confirm that the correct template was targeted by the primer pair selected for each gene. Semiquantitative RT–PCR was performed in triplicate to confirm the expression results, and a representative image of each agarose gel is shown.

Immunoblotting. A human non-pigmented ciliary epithelial (NPCE) cell line was provided by M. Coca-Prados (Yale School of Medicine); a human trabecular meshwork (HTM) cell line was purchased from PromoCell; and a human cervical adenocarcinoma cell line (HeLa S), a human breast adenocarcinoma cell line (MCF-7), and a human embryonic kidney epithelial cell line (HEK293) together with a human retinal pigment epithelial cell line (APRE-19) were obtained from the American Type Culture Collection. All cell lines were tested for mycoplasma and were found to be negative. Cell lysates were generated by lysing individual cell lines with lysis buffer (50 mM Tris-HCl, pH 8, 150 mM NaCl, 1.0% Nonidet P-40, 0.5% deoxycholate, 0.1% SDS, 0.2 mM sodium orthovanadate, 10 mM sodium fluoride, 0.4 mM EDTA, and 10% glycerol). Proteins were resolved by SDS–PAGE and transferred to HyBond-C Extra nitrocellulose membranes (Amersham Life Science). Membranes were blocked in 5% nonfat milk with 10% BSA and 0.1% Tween-20 in Tris-buffered saline (20 mM Tris-HCl, pH 7.6 and 150 mM NaCl) for 1 h before incubation with antibody to choline acetyltransferase (1:500 dilution) from Pierce (PA1-9027; RI); antibody to ependymin-related protein 1 (zebrafish) (EPDR1) (1:500 dilution) from antibodies-online (AA 38-225); antibody to GLIS3 (1:250 dilution) from Sigma-Aldrich (HPA056426); antibody to FERMT2 (1:250 dilution) from Sigma-Aldrich (HPA040505); antibody to DPM2 (1:250 dilution) from Sigma-Aldrich (SAB1104864); antibody to FAM102A (1:250 dilution) from Novus Biologicals (NBP1-88808); antibody to PIP5KL1 (1:250 dilution) from Novus Biologicals (NBP2-29992); and antibody to GAPDH (1:50,000 dilution) from Santa Cruz Biotechnology (sc-25778). Blocking and blotting with antibodies were performed in 5% nonfat milk with 10% BSA and 0.1% Tween-20 in PBS for 1 h each. Horseradish peroxidase (HRP)-conjugated secondary antibodies (GE Healthcare Biosciences) were applied to detect the bound primary antibodies, and signal was visualized with Luminata Forte Western HRP substrate (Millipore).

Immunofluorescence confocal microscopy of tissue sections. Three archival human enucleated eye globes from Singapore (Singapore General Hospital–SNEC Ophthalmic Pathology Service, SGH Department of Pathology) were retrieved for immunofluorescence analysis as normal controls. Ethical approval was provided by the Singapore Health Services Centralized Institutional Review Board. These globes were enucleated for other pathological diagnoses and did not have any intraocular disease. Immunofluorescence analysis was performed according to our previously published protocol[6]. Briefly, paraffin sections were cut at 4 μm and fished onto coated slides, before being dewaxed. Antigen retrieval was performed using Leica Bond ER2 solution for 20 min at 100 °C. Tissue sections were then blocked using 10% FBS and 0.1% Tween-20 in PBS with 1× penicillin-streptomycin for 1 h at room temperature. All primary antibodies were diluted by 1:100 with blocking buffer and incubated with sections overnight at 4 °C. Sections were subsequently labeled with FITC-conjugated (1:300 dilution) anti-mouse, anti-rabbit, or anti-goat secondary antibody (Jackson Laboratories), followed by application of Vectashield with DAPI (Vector Laboratories). Stained histology sections were then coverslipped and stored in the dark at 4 °C. Images were acquired with a Leica TCS SP8 confocal microscope (Leica Microsystems) at the Advanced Bioimaging Core at the Academia, Singapore Health Services.

47. Dunstan, S.J. *et al.* Variation at *HLA-DRB1* is associated with resistance to enteric fever. *Nat. Genet.* **46**, 1333–1336 (2014).
48. Verhoeven, V.J. *et al.* Genome-wide meta-analyses of multiancestry cohorts identify multiple new susceptibility loci for refractive error and myopia. *Nat. Genet.* **45**, 314–318 (2013).
49. Al Olama, A.A. *et al.* A meta-analysis of 87,040 individuals identifies 23 new susceptibility loci for prostate cancer. *Nat. Genet.* **46**, 1103–1109 (2014).
50. Kiryluk, K. *et al.* Discovery of new risk loci for IgA nephropathy implicates genes involved in immunity against intestinal pathogens. *Nat. Genet.* **46**, 1187–1196 (2014).

doi:10.1038/ng.3540